Biomass and Bioenergy 182 (2024) 107059

Contents lists available at ScienceDirect

Biomass and Bioenergy

journal homepage: www.elsevier.com/locate/biombioe

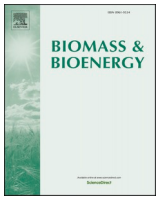

Supercritical water gasification of heavy metal contaminated plants with focus on separation of heavy metal contaminants

Julian Dutzi *, Nikolaos Boukis, Jörg Sauer

Institute of Catalysis Research and Technology (IKFT), Karlsruhe Institute of Technology (KIT), 76344, Eggenstein-Leopoldshafen, Germany

ARTICLE INFO

Keywords:
Supercritical water
Biomass
Gasification
Process design
Heavy metals

ABSTRACT

Soil and groundwater contaminated with heavy metals pose a threat to animals and humans. The use of plants by phytoremediation can help to free the soil and groundwater from the pollutants, but these plants will then become contaminated themselves. The aim of the present work is the energetic utilization of contaminated biomass and the separation of contaminants e.g. heavy metals. This is achieved by gasification of the contaminated biomass under conditions of supercritical water in a continuous laboratory plant. The separation of heavy metal contaminants like zinc, manganese or iron by process-integrated salt separation is necessary to avoid secondary contamination. Reed Canary Grass, Napier Grass and grapevine plants were gasified. Plant type had no effect on gasification efficiency or heavy metal removal. A mean carbon gasification efficiency of 58.3 % was achieved. In all cases, the reactor effluent was free of heavy metal contamination. The general ability to separate salts and heavy metals by salt separation was demonstrated (up to 35 % of heavy metal species detected in the salt brine). The separation is strongly dependent on the preheating temperature (increase in separation of salts when increasing preheating temperature from 460 to 550 °C) and needs to be further improved to avoid the formation of solid deposits in the reaction system. Excessive solid deposition, consisting of coke, salts and corrosion products, limited the experimental duration.

1. Introduction

Due to the careless handling of harmful substances in the past decades, pollutants like heavy metals have been distributed in air, water and soil. The groundwater and soils have been contaminated by mining, industry, transport and agriculture, which poses a threat to humans and animals that feed of the plants growing on contaminated sites [1,2]. Phytoremediation is a technology that uses plants to remove contaminants from soil, groundwater, and air [3]. Within the H2020 EU-project "ContaminatEd land Remediation through Energy crops for Soil improvement to liquid fuel Strategies" (CERESiS) the phytoremediation (in form of phytoextraction) of soils that are contaminated with heavy metals (e.g. Pb, Zn, Cr, Mn) and organics is investigated. For phytoextraction it is important to dispose or recycle the plants used appropriately to prevent secondary contamination [2,4,5]. The Supercritical Water Gasification (SCWG) process is suitable for this purpose as many studies have shown [2,6–10]. In SCWG, organic pollutants can be decomposed and inorganic pollutants like heavy metal salts can be separated in concentrated form. In addition, a hydrogen- and methane-rich product gas is produced [11], which for example can be converted to Fischer-Tropsch fuels after further purification and conversion steps. SCWG uses supercritical water as reaction medium [12]. The critical point and thus the end of the vapor pressure curve in the phase diagram of water is reached at a temperature of 374 °C and a pressure of 22.1 MPa. In the subsequent supercritical state, no distinction between liquid and gas phase is possible [13]. The dielectric constant is a measure of the polarity of a substance. Under ambient conditions, water has an increased dielectric constant and thus is a polar solvent. When the temperature is increased the dielectric constant of water drops sharply [13]. In the supercritical range, it drops further [14], wherefore supercritical water acts as a nonpolar solvent, gases and organic molecules dissolve well [13,15–17]. It is therefore an interesting reaction medium for homogeneous reactions between organic matter and gases [12]. Inorganic salts dissolve poorly in supercritical water and precipitate [18–20]. In SCWG, biomass molecules are hydrolyzed and the hydrolysis products are further decomposed to gases [14,21,22]. The exact reaction mechanisms for biomass are not known due to its complex structure such as lignin, cellulose, hemicellulose. However,

* Corresponding author.
E-mail address: Julian.Dutzi@kit.edu (J. Dutzi).

https://doi.org/10.1016/j.biombioe.2024.107059
Received 19 April 2023; Received in revised form 7 December 2023; Accepted 10 January 2024

decomposition can generally be described by hydrolyzation (eqs. (1) and (2)) [16,23–26]. The global reaction 2 result from the combination of eq. (1) and eq. (3).

$$C_xH_yO_z + (x - z)H_2O \rightarrow xCO + (x - z + 0.5y)H_2 \quad (1)$$

$$C_xH_yO_z + (2x - z)H_2O \rightarrow xCO_2 + (2x - z + 0.5y)H_2 \quad (2)$$

After formation of gaseous products, the water gas shift reaction and methanation reactions take place (eqs. (3)–(5)) [23,25,27]. The reaction products are mainly H_2, CH_4 and CO_2. CO, C_2 and C_3 components are present to a small extent [10,11,28–31].

$$CO + H_2O \rightarrow CO_2 + H_2 \quad (3)$$

$$CO + 3H_2 \rightarrow CH_4 + H_2O \quad (4)$$

$$CO_2 + 4H_2 \rightarrow CH_4 + 2H_2O \quad (5)$$

In literature many experiments with model compounds like glucose, methanol or ethanol were reported [32–34]. When processing biomass, usually wet biomasses were used like sewage sludge, spent grains or animal manure [14,18,35,36]. As SCWG is conducted with water as a reactant the moisture of these biomasses is no issue, as it for example would be in conventional gasification. In contrary dry biomasses are used in the present study as this is the kind of biomass processed in the CERESiS project. More water is thus needed to create the biomass slurry, but previous work shows that the process effluent could be recycled and thus the amount of fresh water needed decreases drastically [10].

In recent studies the fate of heavy metals in the process of SCWG was investigated in batch reactors [2,9,37–40]. Chen et al. demonstrated that during the gasification of lignite no heavy metals were transferred into the gas phase and only low concentrations in the liquid phase were detected. Most heavy metals were detected in the solid biochar, that formed in the process [9]. Su et al. postulate in the gasification of the hyperaccumulator *sedum plumbizincicola* that the formed biochar helps to absorb the heavy metals, where they form complexes with inorganic components [2]. In the gasification of the same plant Su et al. investigated the influence of alkali catalysts and found that the addition of alkali enhanced the immobilization of heavy metals into the biochar, as these catalysts increase gasification efficiencies and thus reduce the amount of organics in the biochar [37]. Thus, it is easier for heavy metals to complex with inorganics in the biochar and to precipitate [39]. Li et al. discovered that during the gasification of oily sludge longer residence times and higher temperatures were beneficial for the transformation of heavy metals from the liquid to the solid phase [40]. During continuous SCWG the formation of char and coke is unwanted since it can lead to blockage of the flow and decreases the gasification efficiency [41–43]. Since batch processes are of little interest for an industrial application of the SCWG process the separation of heavy metals in a continuous process needs to be investigated. For this purpose, continuous lab-scale SCWG experiments were conducted with subsequent analysis of the produced samples.

2. Materials and methods

2.1. Preparation of Educts

The grasses Reed Canary Grass (lat. *Phalaris arundinacea*) and Napier Grass (lat. *Pennisetum purpureum*) and wooden stems and branches of grapevines were used as biomass sources for the gasification experiments (see Table 1 and Fig. 1). The grapevines were delivered in pieces about 10 cm long, which were milled to a powder using a wood chipper (GE 260, Viking), a mill with a 4 mm sieve (Pulverisette 25, Fritsch), and a mill with a 0.2 mm sieve (Pulverisette 14, Fritsch). For the size reduction of Napier Grass the Pulverisette 14 was sufficient. The biomasses were chosen as they are relevant for the CERESiS project. The CERESiS project strategy is to identify high biomass productivity, low contaminant uptake species suitable for a particular climatic zone, following the results of the BioReGen project [44]. Also, there was a lack of literature on the SCWG of dry biomasses.

Table 1
Origin of biomasses.

Biomass	Napier Grass	Reed Canary Grass	Grapevines
Country of origin	Brazil	England	Italy
Site/main soil issue	Former Cr tannery/Cr	Former landfill/clean soil capping	Vineyard/ pesticides
Delivered Form	Straw	Powder (0.25 mm sieve)	About 10 cm long pieces
Dry Matter / wt.%	89.9	97.4	95.1

The elemental composition and the contamination of the biomasses are presented in Table 2 and Table 3. To create a feed slurry, water was added to the biomass powder to adjust the dry mass to about 8 wt% (up to 20 wt% of dry matter is possible to gasify [28], but higher dry matter content than 8 wt% (value from experience) might lead to plugging in feed tubing as the lab-plant is equipped with quarter-inch pipes). Xanthan was added as a thickening agent (0.5 wt%, based on slurry mass) to prevent phase separation, and KOH (5000 mg K+/kg feed slurry) was added as a homogeneous catalyst. KOH enhances the water gas shift reaction, increases H_2-yield and weakens the intermolecular bonds of the biopolymers due to its alkaline character (pH = 9.3 in feed), which increases decomposition of the macromolecules [45–47].

The components were mixed and thermally pretreated at a temperature of 70 °C for 2 h in a mixer (Thermomix TM31, Vorwerk). Low temperature thermal pretreatment is conducted because part of the organics is solubilized after this pretreatment and thus easier to gasify [48,49]. After cooling, samples of the final slurry were taken to analyze dry matter content and elemental composition.

2.2. Apparatus

The "Laboratory Plant for Energetic Utilization of Agricultural Materials" (German acronym: LENA) at the Karlsruhe Institute of Technology is used for laboratory tests. It is a continuous high-pressure plant that can operate at temperatures up to 700 °C and pressures of up to 30 MPa. The current setup includes a preheater, a salt separation unit, and a gasification reactor (see Fig. 2). The dimensions of the preheater and reactor can be seen in Table 4. The set temperatures of the preheater are such that the reaction medium reaches its supercritical state. Salt separation occurs downstream of the preheater using a T-fitting, where inorganic compounds are separated from the biomass slurry due to their low solubility in supercritical water. The salts (and heavy metals) are supposed to drop down vertically into the salt brine at the T-fitting (separation by gravity) while the organics are transported sideways to the gasification reactor (a schematic drawing can be seen in Ref. [10]). A small amount of the salt brine is semi-continuously separated in a defined interval by two needle valves that act as a sluice (they open 20 ms apart). The salt brine is immediately depressurized and collected in a glass container. Since only a small amount of liquid is separated (about 3–5 g per sluice operation) the pressure in the lab-plant is not significantly affected by this.

Gas meters (Ritter GmbH) and scales (Soehnle GmbH) are used to quantify the products of the experiments, positioned in the low-pressure part of the lab-plant. Liquid and gas samples are taken at regular intervals form a glass container in the low-pressure part of the plant during the experiment to ensure a steady-state operating condition. The system is pressurized and heated using a HPLC pump and a process control system. A preliminary test using an ethanol solution is run the day before the main experiment to bring the system into liquid-gas equilibrium (dead volumes of the plant are filled with a gas mixture similar to the gas produced by biomass gasification) and to check for leaks. The feed slurry

Fig. 1. Gasified biomasses as delivered (left to right: grapevines, Napier Grass, Reed Canary Grass).

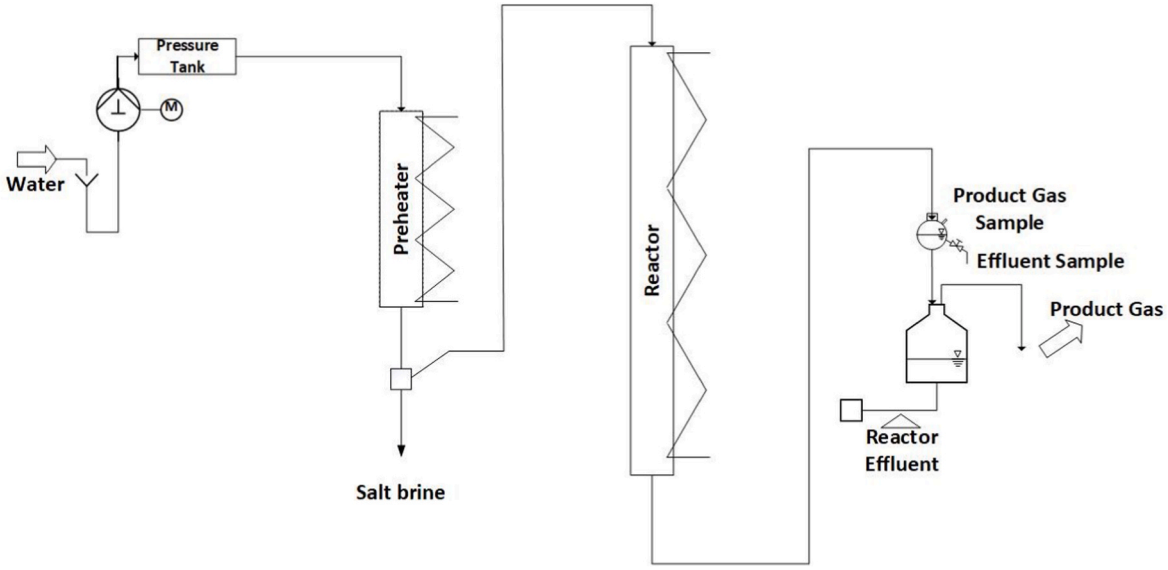

Fig. 2. High-pressure lab-plant for the gasification of biomass.

Table 2
CHNS analysis of biomasses, based on dry weight (in wt.%).

Biomass	C	H	N	S
Napier Grass	43.2	6.00	1.0	0.200
Reed Canary Grass	48.9	7.46	<0.3	0.090
Grapevines	47.1	4.47	1.2	0.003

is stored in a tank and indirectly pumped into the system by a piston using a HPLC pump.

In total seven experiments were conducted (see Table 5). During the experiments the pressure was 28 MPa and the temperature of the SCWG reactor was 650 °C. Three different plants were processed. In addition, three different preheating temperatures and three different flow rates were set for the gasification of Reed Canary Grass. The duration of the experiments was limited by the available amount of feed slurry (some experiments were ended prematurely due to blockage of the flow). Each experiment was conducted once due to the limited time and resources and high effort it takes to prepare the experimental setup.

2.3. Analysis

Gas samples of the product gas are analyzed using a gas chromatograph (5890 series II plus by Hewlett Packard Inc.) with a fused silica capillary column (Carboxen 1010 PLOT 30 m, SUPELCO). The volume fractions of various gas components, including H_2, CO, CH_4, CO_2, C_2H_4, C_2H_6, C_3H_8 and C_3H_6, are determined using a thermal conductivity and flame ionization detector. Sampling is done every 30 min. Liquid samples are collected from effluent streams at regular intervals for analysis of Total Carbon (TC) by combustion and Total Inorganic Carbon (TIC) by acid extraction in a TOC-analyzer (DIMATOC 2100, DIMATEC). Total Organic Carbon (TOC) is determined by subtracting TIC from TC. Trace

Table 3
Heavy metal contamination of biomasses (in ppmw).

Biomass	Pb	Ni	Zn	Cd	Cr	Mn	Fe
Napier Grass	126.18	12.63	49.93	1.05	27.25	70.83	348.10
Reed Canary Grass	0.50	0.60	37.00	<0.10	0.90	490.00	61.00
Grapevines	0.05	0.06	26.61	<0.10	0.15	50.40	42.80

Table 4
Dimensions of preheater and reactor.

	Preheater	Reactor
Material	Inconel 625 with SS 316 Liner	Inconel 625
Length/mm	750	1800
Inner Diameter/mm	3.20	8.00
Electric Heating	3 spiral heaters	6 rod heaters

Table 5
Process parameters of conducted experiments.

Experiment Number	Feed	Duration h	$T_{Preheater,max}$ °C	Flow rate g h^{-1}
1	Napier Grass	4.50	500	700
2	Grapevines	5.75	500	700
3	Reed Canary Grass	6.50	500	700
4	Reed Canary Grass	3.50[a]	460	700
5	Reed Canary Grass	3.92[a]	550	700
6	Reed Canary Grass	6.25	500	500
7	Reed Canary Grass	0.25[a]	500	300

[a] Premature ending of the experiments due to blockage of the flow.

elements, including Al, Ca, Cd, Cr, Cu, Fe, K, Mg, Mn, Mo, Na, Ni, Pb, S, Si, and Zn, are determined using ICP-OES (Inductively Coupled Plasma - Optical Emission Spectrometry) in an Agilent 725 spectrometer. Solid samples are analyzed using SEM-EDS (Scanning Electron Microscope - Energy Dispersive X-ray Spectroscopy) in a GeminiSEM 500 (Carl Zeiss AG). A sample of the biomass feed is dried at 105 °C in an oven for 24 h, and afterwards the C, H, N, and S contents are analyzed in the element analyzer vario EL cube (by Elementar Analysensysteme GmbH), and the trace elements are analyzed via ICP-OES.

2.4. Data interpreation

Three key figures will be discussed to evaluate the experimental data: carbon efficiency, residence time and TOC-conversion. The analysis conducted according to section 2.3 is used for the calculation of the key figures. The TOC-conversion TOC_{conv} compares the amount of TOC in the effluent streams $TOC_{Effluents}$ to the TOC content of the feed TOC_{Feed} (eq. (6)) and therefore is an indicator of the purity of the effluents. The part of the TOC that is not present in the effluent streams was either transformed to gaseous products or to dissolved inorganic compounds or formed solid deposits in the system. The higher TOC_{conv} is, the lower the TOC content in effluents is and thus the better the waste water quality is.

$$TOC_{conv} = \frac{TOC_{Feed} - TOC_{Effluents}}{TOC_{Feed}} = 1 - \frac{\dot{m}_{R,effluent} * TOC_R + \dot{m}_{S,effluent} * TOC_S}{\dot{m}_{Feed} * \alpha} \quad (6)$$

α Carbon concentration in the feed (wt.%)
$\dot{m}_{Feed}$ Feed mass flow (g/h)
$\dot{m}_{R,effluent}$ Mass flow of reactor effluent (g/h)
$\dot{m}_{S,effluent}$ Mass flow of salt brine (g/h)
TOC_R TOC content of reactor effluent (mg/g)
TOC_S TOC content of salt brine (mg/g)

The carbon efficiency *CE*, a measurement of the gasification efficiency, is defined as:

$$CE = \frac{C\ in\ Product\ Gas}{TOC\ in\ Feed} = \frac{\sum \beta_i * x_i * \frac{\dot{V}_{Gas} * p}{R * T} * M_c}{\dot{m}_{Feed} * \alpha} \quad (7)$$

x_i Concentration of component 'i' in the gas product (vol%)
β_i Number of carbon atoms of component 'i' in the gas product
M_c Molar mass of carbon (g/mol)
p Pressure (Pa)
R Universal constant of gases (J/(K*mol))
T Temperature (K)
$\dot{V}_{Gas}$ Gas flow under ambient conditions (l/h)

To calculate the residence time τ (eq. (8)) in the reactors the mass content of the reactor at given temperatures and thus given densities has to be calculated. To determine the density at a given point in the reactor the temperature profile is divided in section of length l (defined by the many thermocouples installed). In each section the average temperature is calculated and used for determining the density in this section. The total residence time is calculated by adding up the residence times in the different sections. Due to the high water content in the reaction mixture the density of the mixture is assumed to be equal to the density of water.

$$\tau = \frac{\pi * \left(\frac{d}{2}\right)^2 * l * \rho_{H_2O}}{\dot{m}_{Feed}} \quad (8)$$

d Inner diameter of the reactor (m).
l Length of section with constant temperature (m).
ρ_{H_2O} Density of water at given temperatures (kg/m^3).

3. Results and discussion

3.1. Influence of biomass type

To investigate the influence of the dry biomass type on the process of SCWG three different dry plants were processed. Two grasses, Napier Grass and Reed Canary Grass, and a plant with wooden stems and branches, grapevines, were gasified (see Table 6). The mean steady-state carbon balance was 77 % with a standard deviation of 4.3 % in all experiments, as not all carbon could be detected either in gas or liquid effluent and solid deposits formed. Obviously, solids remain in the tubing of the plant causing fouling. This leads to premature end of several experiments, mechanical cleaning of the plant had to be performed frequently. The experiments for comparison of the different biomasses (experiments 1, 2 and 3) were finished according to plan.

The feed composition regarding the CHNS content and the content of the main salt building elements can be seen in Table 7. There are some differences between the feed compositions, especially the potassium content of the biomass slurry of Napier Grass is higher than the other two kinds of feed. This is due to the high potassium content of the biomass Napier Grass, which has been described in literature [50,51].

Minor differences between the plants regarding carbon efficiency were noticed (experiments 1, 2 and 3) (see Table 6). The mean CE for all plants is 58.3 % with a maximum deviation of 3.1 %. The CE is therefore not influenced by the kind of dry plant that was processed in the present experiments. D'Jesus et al. also noticed only small differences in CE

Table 6
Results of the gasification experiments.

Experiment Number	Feed	CE %	TOC-conversion %	TOC content in effluent mg kg^{-1}
1	Napier Grass	60.45	78.03	3933
2	Grapevines	55.18	86.20	3027
3	Reed Canary Grass	59.14	83.83	3204
4	Reed Canary Grass	67.35	89.69	3765
5	Reed Canary Grass	63.38	85.66	3310
6	Reed Canary Grass	61.92	89.13	2821
7	Reed Canary Grass	–	–	–

Table 7
Content of CHNS and main salt building elements in the feed slurry in wt.% (based on dry matter).

Experiment Number	Feed	C	H	N	S	K	Ca	Mg	Si	P
1	Napier Grass	39.3	5.6	0.9	0.2	6.90	0.45	0.03	0.88	0.12
2	Grapevines	43.6	5.7	0.5	<0.1	4.13	1.53	0.10	0.46	0.13
3	Reed Canary Grass	39.6	5.5	0.4	0.1	4.68	0.29	0.08	2.27	0.13

when gasifying clover grass (44.9 wt% C in biomass) and corn starch (44.4 wt% C in biomass) in a similar lab-plant [52]. Thus, when biomasses with similar elemental composition are gasified (similar carbon content) the CE does not seem to be significantly influenced by the type of plant. A small difference in the TOC content of the reactor effluent is visible. The TOC-conversion is 78 % for Napier Grass, 84 % for Reed Canary Grass and 86 % for grapevines. Since the TOC conversion compares the amount of TOC that is contained in the effluents with the TOC content of the feed it is an indicator of the effluent purity. During experiment 1 with Napier Grass a 20% higher TOC content in the effluent is visible than in the other two experiments although CE is roughly the same. This can be explained by the formation of solids during the experiments 2 and 3 with Reed Canary Grass and grapevines. After each experiment the reactor and the preheater are opened and checked for solid deposits. After the experiment with Napier Grass no solid deposits were found in the system. After the other two experiments solid deposits were found at the top of the SCWG reactor (300–500 mm from the top, where a temperature of 500 °C was set). The carbon contained in these solid deposits can not be gasified and is not contained in the reactor effluent and therefore the TOC content of the experiments with Reed Canary Grass and Grapevines was lower than in the experiment with Napier Grass even though the carbon efficiency and therefore the amount of gas produced was roughly the same. The gas composition is also not influenced by the kind of dry plant that is processed (see Fig. 3). The mean H_2-content of the product gas is 31 vol% with only little deviation. The most visible difference can be seen when comparing the CO_2 and CH_4-contents of the product gas of Napier Grass and Grapevines. About 4 vol% more CO_2 and 1.5 vol% less CH_4 is contained in the product gas of Napier Grass than in the product gas of grapevines. The methanation reactions seem to take place in a slightly greater extend in the case of Napier Grass. Methanation reactions are kinetically limited and therefore longer reaction times result in an increased CH_4-yield [29,53,54]. The flow rate was set at 700 g h^{-1} during all three experiments and thus the residence times were the same initially. As mentioned before, solid deposits occurred during the gasification of grapevines. These solid deposits reduce the free diameter of the reactor and so the residence time decreases over the course of the experiment. This could be a possible reason for the small differences in gas composition.

As the heavy metal contamination (see Table 3) of the biomasses is rather low, the gasification process is presumably not significantly influenced by the heavy metals. Thus, the achieved gasification results can be transferred to non-contaminated biomasses of the same species.

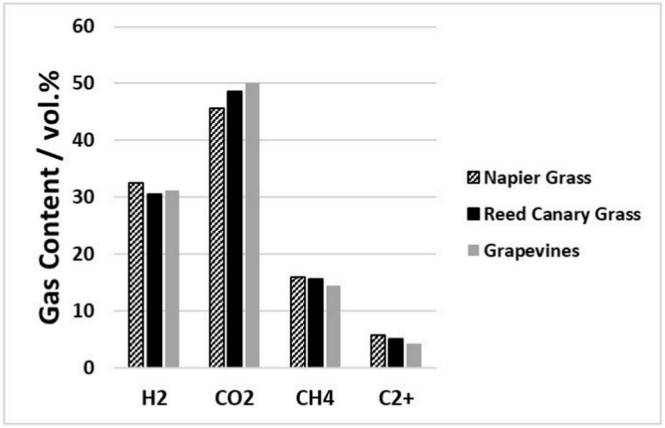

Fig. 3. Gas composition of the gasification of three different feeds.

3.2. Influence of the preheating temperature

The temperature settings of the preheater are crucial for the separation of salts in the LENA lab-plant. Salts need to be separated from the reaction medium since salts can cause blockage of the flow due to precipitation [55,56] and enhance corrosion rates at T > 500 °C [56–59]. Salts are generally poorly soluble in supercritical water [20] and thus can be separated by precipitation. In binary salt-water systems salts are distinguished between type 1 and type 2 salts [19,60,61]. Type 1 salts are soluble in dense supercritical water and only precipitate when the temperature is further increased, while type 2 salts are almost non-soluble in supercritical water. Downstream of the preheater a T-fitting is located where salts are supposed to be separated by precipitation. Since the T-fitting at which salts are supposed to be separated is not externally heated the reaction medium needs to be preheated sufficiently so the temperature is supercritical at the T-fitting. The salt separation is conducted upstream of the gasification reactor to avoid extensive salt deposition in the reactor. To investigate the influence of the preheating temperature on the separation of salts three different maximum preheating temperatures (460–550 °C) were set. This resulted in the following temperatures at the T-fitting (measurement on the outside) (see Table 8).

To evaluate the quality of salt separation the concentration of relevant salt building elements (Ca, K, Mg, Na, S, Si and P [62–64]) is monitored in the effluents of the lab-plant. During the experiment 4 only a subcritical temperature of 370 °C could be reached at the T-fitting. Thus, the separation of salts based on precipitation does not work. This can be seen when looking at the distribution of the salt building elements (see Fig. 4). Less than 20 %, in most cases even less than 10 % of the salt building elements can be detected in the salt brine. Potassium and sodium are mostly detected in the reactor effluent and the rinse water (after every experiment the system is flushed with water). For all other salt building elements, a big mass balance deficit can be seen. The balance deficit, as mentioned, can be assumed to consist of solid deposits that mainly stayed in the reaction system (some solids were also contained in the salt brine). Solid deposits cannot be quantitively collected and analyzed (due to their inhomogeneities) and therefore cannot be calculated into the mass balance of the elements. After experiment 4 solid deposits were discovered in the top part of the SCWG reactor where a temperature of 500 °C was set. The formation of solid deposits in the reaction system poses a danger to long-time operation of the process.

The increase of the preheating temperature to 500 °C (experiment 3) resulted in a slightly supercritical temperature of 388 °C at the T-fitting. The separation of calcium, sodium and phosphorus into the salt

Table 8
Temperatures of the T-fitting for salt separation.

Experiment Number	$T_{Preheater,max}$ °C	$T_{T\text{-}Fitting}$ °C	Duration of Experiment h
4	460	370	3.5[a]
3	500	388	6.5
5	550	394	3.9[a]

[a] Premature ending of the experiments due to blockage of the flow.

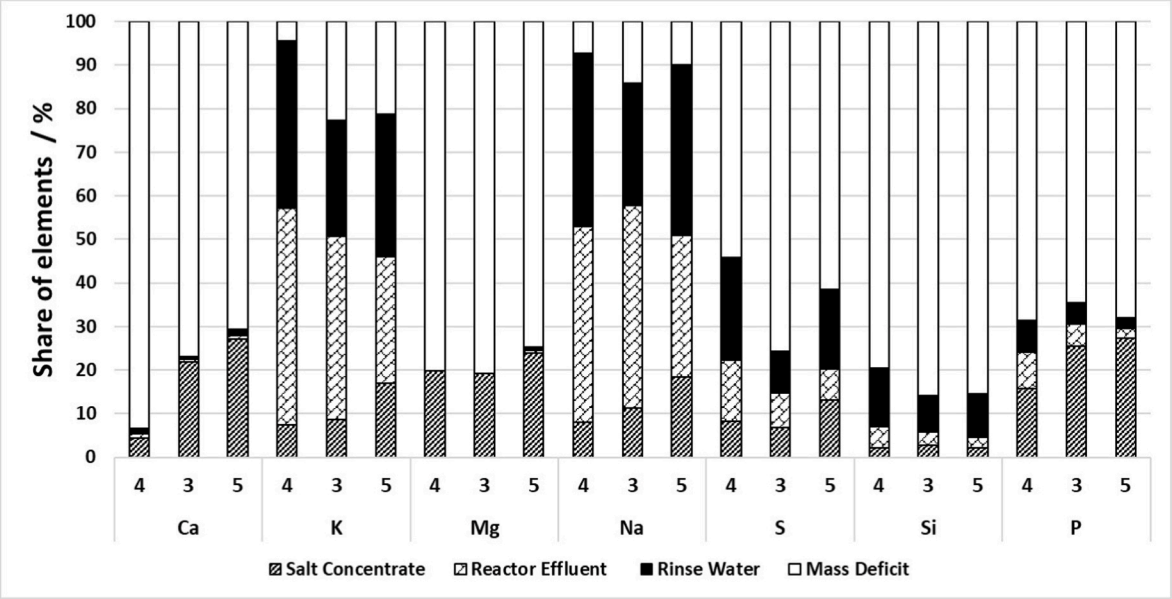

Fig. 4. Share of elements in the liquid effluents of different experiments (4, 3, 5) (feed concentration = 100 %).

separation increased. The separation of the other elements was not influenced by the rise in temperature. As stated earlier, salt separation is influenced by the type of salt. Examples of type 2 salts that could explain the shown behavior of Ca and P could be $CaSO_4$ and Na_3PO_4 [65]. The separation of the other salt building elements was not influenced. These salt building elements might be present in type 1 salt configurations, such as NaCl, K_3PO_4, KCl or K_3SiO_3 [56,65]. The mass deficit of most elements is very large. Similar to the experiment 4, after the experiment 3 solid deposits were discovered in the top part of the reactor where a temperature of 500 °C was set. The qualitative analysis (EDS-analysis) of

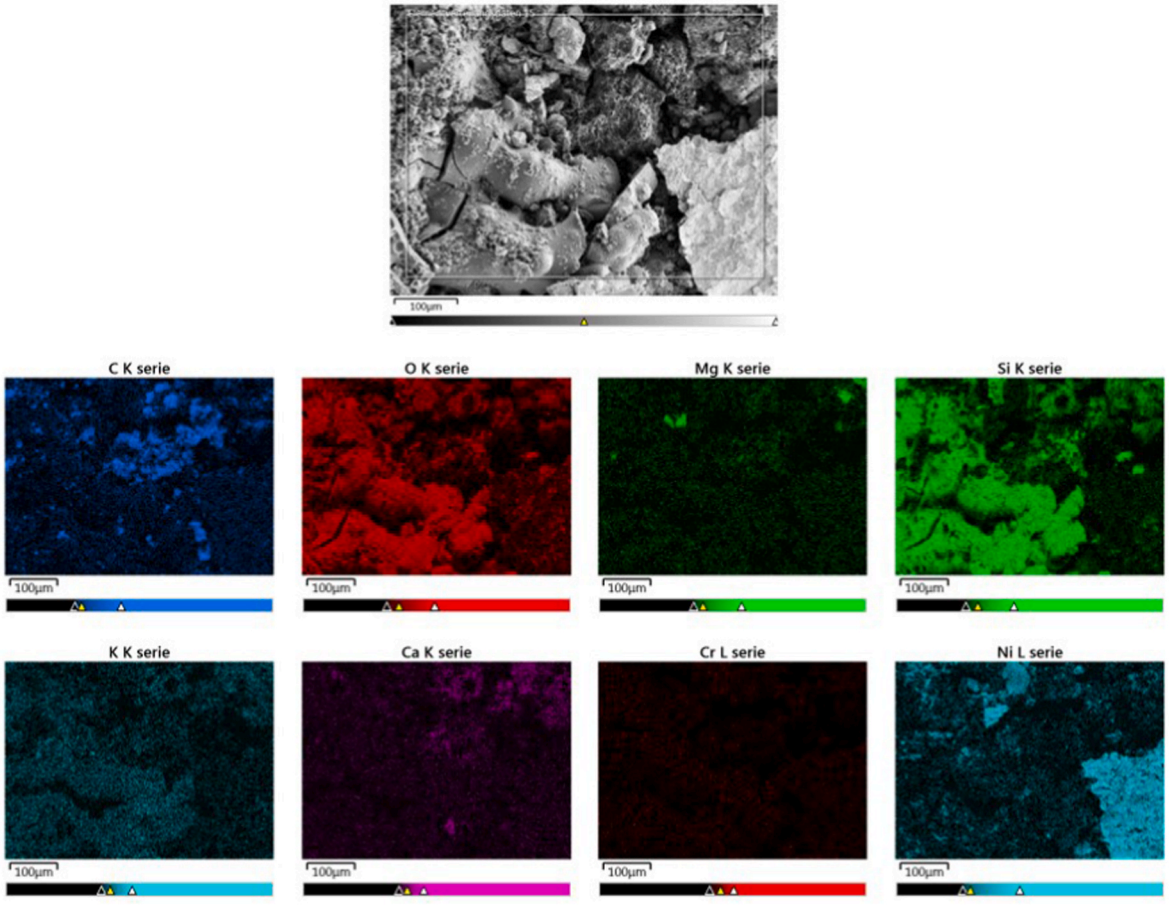

Fig. 5. SEM-EDS analysis of the solid deposits of experiment 3.

the solid deposits of the SCWG reactor (experiment 3) displays a mixture of carbon and salt building elements (see Fig. 5). Especially silicon and potassium can be detected. On the right side of the micro photography a big planar structure consisting of nickel can be seen. This can be assumed to be a corrosion product from the reactor. The reactor is made of the nickel-based alloy Inconel 625. Since salts are known to enhance corrosion rates this shows the importance of a functioning salt separation. The functionality of the salt separation was still not given for the selected process conditions.

In both experiments (experiments 4 and 3) the solid deposits occurred in the section of the reactor where a temperature of 500 °C was set (on the outside of the pipe). An inner temperature measurement in the reaction medium was not possible. Therefore, the reaction temperature has to be estimated based on data given in literature. Due to a relatively big inner diameter of 8 mm in the SCWG reactor a low flow speed results. D'Jesus could not detect any temperature gradients between inside the medium and outside of the pipe in a SCWG reactor with 8 mm inner diameter [66]. In the section where the solid deposits occurred the temperature in the reaction medium can therefore be assumed to be above 450 °C (and below 500 °C). This temperature range seems to be critical for the separation of most salts. This has been experimentally confirmed by Schubert et al. [19]. According to Schubert et al., a temperature of 430 °C is necessary to separate more than 90 % of K_3PO_4 and 470 °C to separate more than 90 % of $Ca(NO_3)_2$ into the salt brine [19]. In experiments 4 and 3, in which a maximum preheating temperature of 460 and 500 °C was set, these temperatures seem not to be reached in the reaction medium within the preheater and thus the precipitation of salts could not take place at the T-fitting. Due to a small inner diameter of the preheater (3.20 mm) and thus higher flow speed a lower maximum temperature of the reaction medium is reached.

A further increase in the preheating temperature to 550 °C (experiment 5) resulted in 394 °C at the T-fitting. Even though this temperature is only 6 °C higher than when the preheating temperature was 500 °C, an improved salt separation can be seen for almost all salt building elements. Almost 30 % of Ca and P can be separated. The separation of K, Na, Mg and S also improves by about 5 %. Solely silicon is not influenced by the increasing temperature. The mass deficit is still very high for most salt building elements (except K and Na). During this experiment solid deposits formed in the preheater, leading to faster plugging even though the salts were separated more efficiently as the inner diameter of the preheater was smaller than that of the reactor. Due to the high maximum preheating temperature of 550 °C the temperature in the reaction medium can be assumed to be higher than 450 °C in the preheater. This resulted in improved salt separation but also in precipitation of salts in the preheater and led to blockage of the flow in the preheater. In Fig. 6 it can be seen that Ca, Mg, Si and K are part of the solid deposit in the preheater.

3.3. Influence of residence time

To investigate the influence of the residence time on CE and the formation of solid deposits during the gasification of Reed Canary Grass three different throughputs were set (see Table 9). Experiment 7 did not reach a steady state and therefore it can not be considered in the evaluation of the trend of CE and TOC. For the other two experiments (3 and 6) CE only slightly rises with increasing residence time (17–24 s) (see Table 9). Generally, it is known that CE rises strongly with increasing residence time [53,67,68]. This cannot be observed in the present

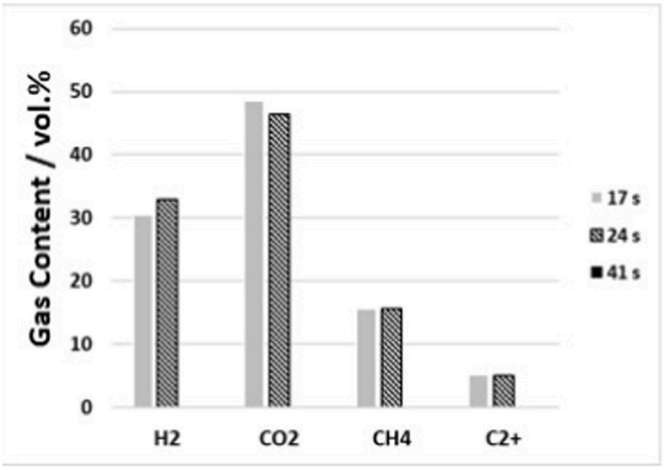

Fig. 7. Steady state gas composition for three different residence times in the SCWG reactor (T > 600 °C), no steady state reached for the mean residence time of 41 s.

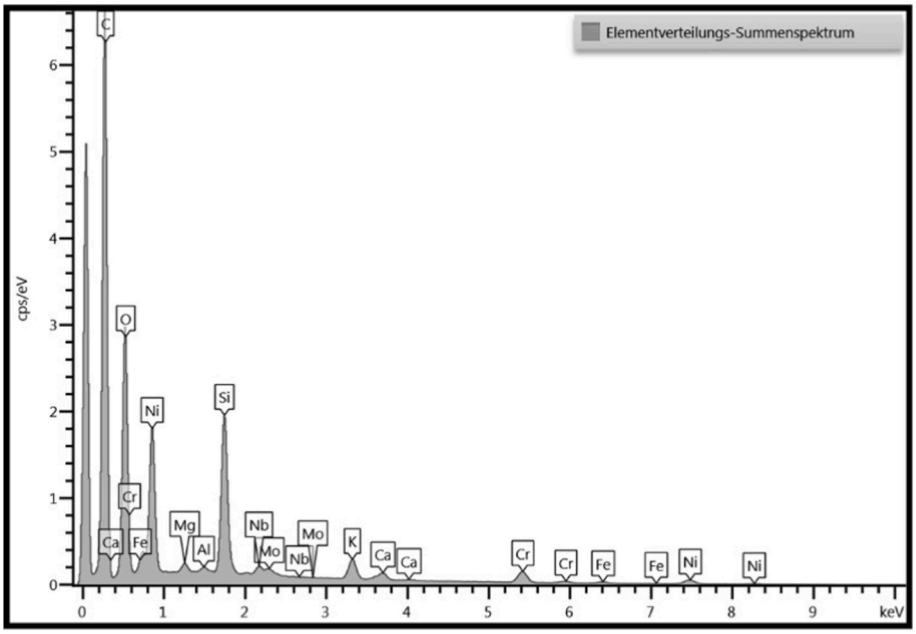

Fig. 6. Elemental spectrum of a sample of solid deposits in the preheater.

Table 9
Residence time and salt separation temperature of three different experiments.

Experiment Number	Duration h	Flow rate g h^{-1}	$\tau_{Preheater}$ s	$\tau_{Reactor\ (T>600\ °C)}$ s	$T_{T\text{-}Fitting}$ °C
3	6.5	700	4.6	17	388
6	6.25[a]	500	7.4	24	400
7	0.25[a]	300	12.4	41	420

[a] Premature ending of the experiments due to blockage of the flow.

experiments. A possible reason for this could be the formation of solid deposits in the SCWG reactor (as stated in section 3.2). This assumption can be made since the TOC content of the effluent decreases while CE only rises slightly with increasing residence time. Experiment 6 had to be finished prematurely due to blockage of the flow in the SCWG reactor. After experiment 3 solid deposits were also detected in the same part of the reactor but they did not lead to blockage of the flow. Therefore, more solid deposits were formed during experiment 6. A lower flow speed and thus higher residence time in the temperature range of 450–500 °C seems to be disadvantageous for the chemistry of SCWG towards gases and favors the formation of solid deposits. Faster heating to the desired temperature of 650 °C should be implemented since tar and char production are significantly influenced by the heating rate [69]. This might avoid coke formation and additionally enable better salt separation as the salts seem to deposit in a temperature range of 450–500 °C, which so far has not been reached at the salt separation T-fitting.

The gas composition is not significantly influenced by the increase of the residence time (see Fig. 7). It is well known from literature that the CH_4 rises with increased residence time due to the kinetic limitation of the methanation reactions [29,53,54]. This cannot be observed in this set of experiments. A slight increase of H_2 can be seen when the residence time is increased from 17 to 24 s. This effect has been reported by other authors [68,70]. As stated above, experiment 7 did not reach steady state operation due to blockage of the flow. Solid deposits blocked the flow in the preheater. As described in section 3.2, a temperature of above 450 °C in the reaction medium seems to be critical for the formation of solid deposits that consist of coke and salts (see Figs. 5 and 6). In order to achieve higher residence times, the throughput was reduced from 700 to 300 g h^{-1}. This resulted in reduced flow speed in the preheater. Due to the reduced flow speed higher temperatures can be reached in the preheater. An indicator for this is the temperature at the salt separation (T-fitting) downstream of the preheater (see Table 9). When a throughput of 700 g h^{-1} was set the temperature was 388 °C but when the throughput was 300 g h^{-1} it was 420 °C at the T-fitting. Therefore, it can be assumed that the critical temperature range of T > 450 °C was reached within the preheater (assuming some thermal losses in the not heated part of the plant) and led to precipitation, combined with a low flow speed. This explains why solid deposits formed in the preheater and blocked the flow after a short time and a further increase in residence time could not be investigated.

To achieve higher residence times a larger reactor should be implemented in future experiments instead of reducing the throughput. In that way consistent temperatures of the reaction medium will be ensured. This will avoid the change of a second parameter – the temperature profile – when the residence time is changed and thus clear correlations between residence time and CE can be determined.

3.4. Separation of heavy metals

In batch SCWG experiments with contaminated biomasses most heavy metals remain in the forming biochar and only low concentrations are measured in the liquid effluents [2,9,37]. The suggested separation mechanism by Lin et al. is that the heavy metals compound with inorganic components in the reaction mixture and precipitate due to low solubility in supercritical water [39]. Therefore the addition of inorganic components in alkali metal catalysts (K, Ca, Na) promotes the precipitation [37]. Since batch experiments are not relevant for an industrial application of SCWG in this study the experiments were conducted in a continuous lab-plant. KOH was added to the feed as a homogeneous catalyst. To evaluate the separation of heavy metals the liquid effluents were analyzed. For many heavy metals the content was below the detection limit in the liquid effluents. Ni, Co, As, Pb, Cd, Cu and Sn were not detectable in the effluents. Most experiments (experiments 3 to 7) were conducted with the grass Reed Canary Grass. The heavy metal contamination of this plant from highest to lowest is Mn > Fe > Zn > Cr > Ni > Pb > Cd (for exact concentration see Table 3). The mean content of detectable heavy metals is displayed in Fig. 8.

Only three heavy metals are detectable, Mn, Fe and Zn. The content of the other heavy metals was below the detection limit in the feed slurry and therefore also in the effluents. About 21.5 ± 8 % of Mn, that was in the feed slurry, can be detected in the salt brine. 9.0 ± 1 % of Fe and 10.2 ± 3.6 % of Zn are detected in the salt brine. Less than 0.6 % of the heavy metals can be detected in the reactor effluent and none in the rinse water. The separation of contaminants is based on the precipitation in supercritical water due to low solubility. Since heavy metals are only detected in the salt brine it can be assumed that they form heavy metal-salt-compounds as proposed by Lin et al. [39] and precipitate into the salt brine.

Most of the amount of the heavy metals that are fed into the system cannot be found in liquid effluents. One reason for this are the detection limits of the analysis method (ICP-OES). The heavy metals might for example be so diluted that they are not detected in the rinse water even though it might contain some. Another reason is the formation of solid deposits in the reaction system which are also insoluble in water under ambient conditions. As described in section 3.2 solid deposits form in the system, especially in the SCWG reactor. These solid deposits also contain heavy metals as can be seen in Fig. 9, in this part of the solid deposit Cr, Ni and Fe.

Only one experiment (experiment 1) was conducted with Napier Grass and one with grapevines (experiment 2).

In grapevines Mn, Fe and Zn make up the biggest part of the heavy metal contaminants. Only 3.5 % of the fed Fe can be detected in the effluents (see Fig. 10). 35 % of Mn and 10 % of Zn can be detected in the salt brine. The heavy metals show a similar behavior as in the gasification of Reed Canary Grass. Fe, Pb, Mn and Zn are the main contaminants of Napier Grass. In the experiment with Napier Grass almost no heavy metals were detected in the effluents (see Fig. 11) but as seen in the other gasification experiments the only detected heavy metals were found in the salt brine. Little to none were found in the reactor effluent or the rinse water. Pb was not detected at all.

In batch experiments it was proposed that the heavy metals formed compounds with inorganics and precipitated. Due to the detection of heavy metals in the salt brine this mechanism seems to be justified. As described in section 3.2 the salt separation of this lab-plant does not work sufficiently under the selected conditions. In the future an improved salt separation should reduce the formation of solid deposits or transport the solids towards the salt brine and improve the precipitation of salts and thus also of heavy metals into the salt brine. Even though, the salt separation was not optimal in the conducted experiments, it is shown that in principle the separation of heavy metals from the reaction mixture is possible during continuous SCWG. It can also be noted that under the chosen conditions the reactor effluent can be considered free of heavy metals (concentration below quantification limit) and therefore can be treated as not contaminated. This is the most important aspect as this effluent would either be discharged or recycled to create new feed in a commercial application. In the framework of the CERESiS project a novel procedure for the separation of the heavy metals from the salt brine is currently under development (results not yet reportable) and thus the separation of heavy metals into the salt brine is the desired pathway.

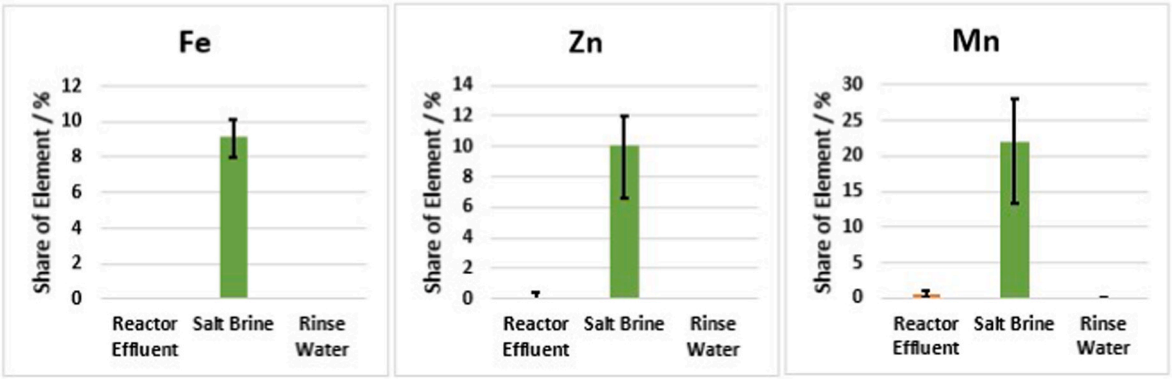

Fig. 8. Mean content of heavy metals in the effluents of the experiments with Reed Canary Grass (100 % = feed concentration).

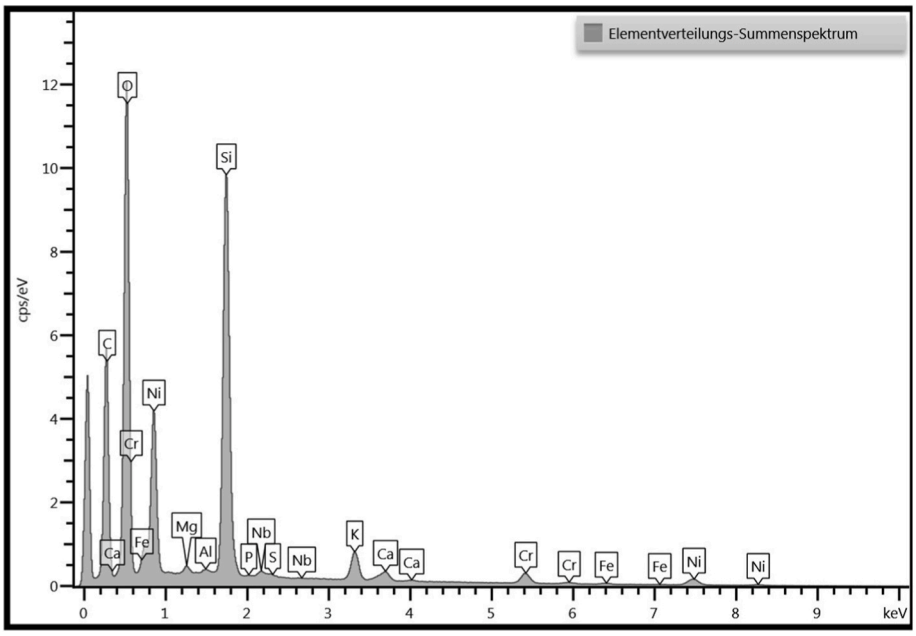

Fig. 9. Elemental composition of solid deposits in experiment 1.

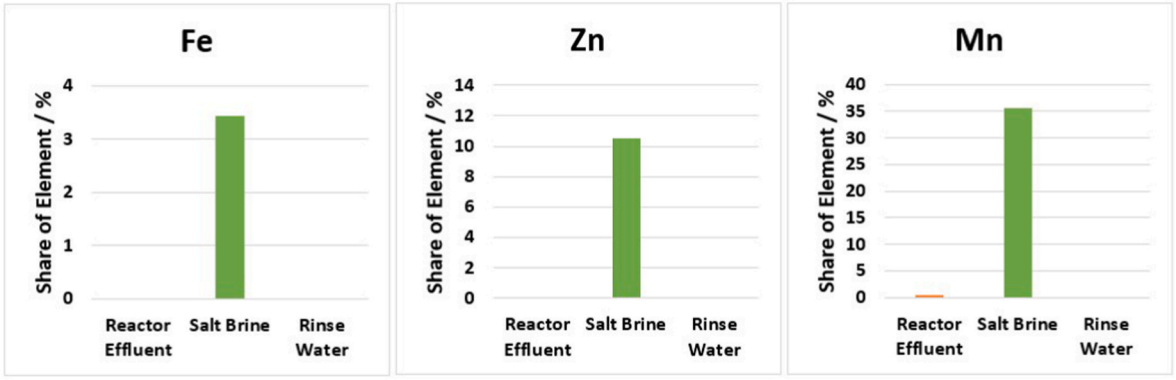

Fig. 10. Content of heavy metals in the effluents of the experiment with grapevines (100 % = feed concentration).

4. Conclusion

It was demonstrated that the separation of heavy metal contaminants from biomasses was possible with a process integrated salt separation. The carbon efficiency *CE* and the capability of heavy metal separation were not influenced by the type of plant that was gasified (Reed Canary Grass, Napier Grass, grapevines). CE was 58.3 % with a maximum deviation of 3.1 % for all three plants. The reactor effluent was heavy metal-free under all conditions tested (concentrations below quantification limit). Salt and thus heavy metal separation strongly depend on

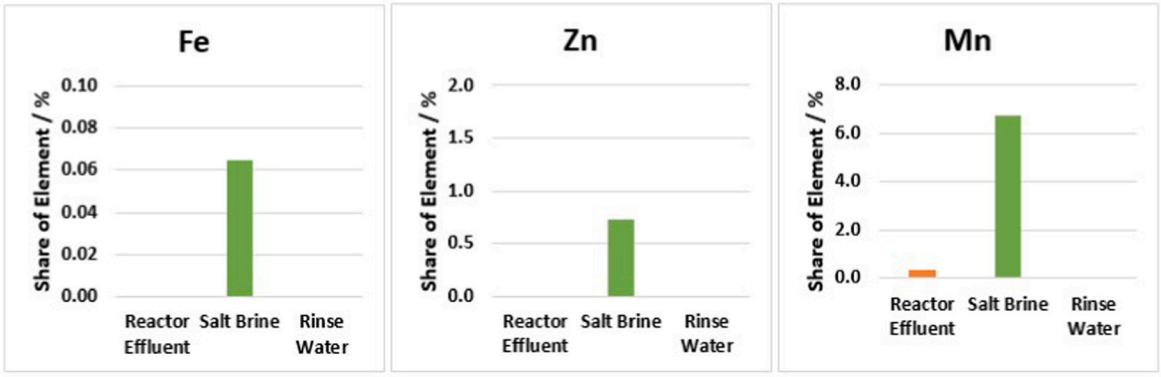

Fig. 11. Content of heavy metals in the effluents of the experiment with Napier Grass (100 % = feed concentration).

the preheating temperature prior to salt separation. Salt separation temperatures of 394 °C or lower are not sufficient for complete salt separation. This led to formation of solid deposits containing coke, salts and heavy metals in the reaction system. Due to the relatively low CE, the formation of solid deposits and the remaining TOC in the effluent, the realization of the SCWG process in this process design is not recommendable, further process development is necessary. To avoid blockage of the flow and enable long-time runs further improving of the salt separation, especially the temperature profile, needs to be done in future experiments. The geometry of the salt separation T-fitting might show potential for optimization. A possible optimization could be a sharper redirection of the flow. In future experiments an inner temperature measurement, which is very difficult due to the high pressure and high temperature environment, should also be completed to accurately determine the temperature of salt precipitation. The set temperature of the preheater should be in such way that the salt separation temperature can then be reached right before the T-fitting. At the same time the flow speed of the preheater needs to be high enough to transport precipitating salts to the salt brine and to avoid blockage of the preheater. Additionally, faster heating rates should be applied to reduce solid coke deposit formation.

Funding

This research work was funded by the H2020 EU-Project CERESiS (Grant-Agreement-Nr.: 101006717).

CRediT authorship contribution statement

Julian Dutzi: Conceptualization, Data curation, Formal analysis, Investigation, Validation, Visualization, Writing – original draft. **Nikolaos Boukis:** Conceptualization, Funding acquisition, Methodology, Resources, Validation, Writing – review & editing. **Jörg Sauer:** Supervision, Validation, Writing – review & editing.

Declaration of competing interest

The authors declare no conflict of interest.

Data availability

Data will be made available on request.

Acknowledgments

The authors would like to thank Mrs. E. Hauer for the contributions to the experimental work and Mr. K. Weiss, responsible for most of the mechanical work, for his contributions. Special thanks to the University of Strathclyde, the University of Tuscia and the Universidade Federal de Goias for providing the biomasses. The authors would like to thank Dr. D. Katsourinis and Prof. A. Rentizelas for the coordination of the H2020-project CERESiS.

References

[1] J.O. Nriagu, Global inventory of natural and anthropogenic emissions of trace metals to the atmosphere, Nature 279 (1979) 409–411.
[2] W. Su, P. Liu, C. Cai, H. Ma, B. Jiang, Y. Xing, et al., Hydrogen production and heavy metal immobilization using hyperaccumulators in supercritical water gasification, J. Hazard 402 (2021) 1–9.
[3] C. Baskar, S. Baskar, S. Dhillion, Biomass Conversion, Springer-Verlag Berlin Heidelberg, 2012.
[4] H. Jiang, R. Yan, C. Cai, X. Chen, F. Zhao, Z. Fan, et al., Hydrothermal liquefaction of Cd-enriched Amaranthus hypochondriacus L. in ethanol-water co-solvent: Focus on low-N bio-oil and heavy metal/metal-like distribution, Fuel 303 (2021) 1–9.
[5] X. Zhu, F. Qian, C. Zhou, L. Li, Q. Shi, S. Zhang, et al., Inherent metals of a phytoremediation plant influence its recyclability by hydrothermal liquefaction, Environ. Sci. Technol. 53 (2019) 6580–6586.
[6] J. Li, J. Chen, S. Chen, Supercritical water treatment of heavy metal and arsenic metalloid-bioaccumulating-biomass, Ecotoxicol. Environ. Saf. 157 (157) (2018) 102–110.
[7] M. Carrier, A. Loppinet-Serani, C. Absalon, F. Marias, C. Aymonier, M. Mench, Conversion of fern (Pteris vittata L.) biomass from a phytoremediation trial in sub- and supercritical water conditions, Biomass Bioenergy 35 (35) (2011) 872–883.
[8] W. Shi, C. Liu, D. Ding, Z. Lei, Y. Yang, C. Feng, et al., Immobilization of heavy metals in sewage sludge by using subcritical water technology, Bioresour. Technol. 137 (2013) 18–24.
[9] G. Chen, X. Yang, S. Chen, Y. Dong, L. Cui, Y. Zhang, et al., Transformation of heavy metals in lignite during supercritical water gasification, Appl. Energy 187 (2017) 272–280.
[10] J. Dutzi, N. Boukis, J. Sauer, Process effluent recycling in the supercritical water gasification of dry biomass, Processes 11 (2023) 797.
[11] A. Kruse, A. Funke, M. Titirici, Hydrothermal conversion of biomass to fuels and energetic materials, Curr. Opin. Biotechnol. 17 (2013) 515–521.
[12] A. Kruse, E. Dinjus, Hot compressed water as reaction medium and reactant properties and synthesis reactions, J. Supercrit. Fluids 39 (2007) 362–380.
[13] A.A. Galkin, V.V. Lunin, Subcritical and supercritical water: a universal medium for chemical reactions, Russ. Chem. Rev. 74 (2005) 21–35.
[14] O. Yakaboylu, J. Harnick, K.G. Smit, W. Jong, Supercritical water gasification of biomass: a literature and technology overview, Energies 8 (2015) 859–894.
[15] A. Loppinet-Serani, C. Aymonier, F. Cansell, Current and foreseeable applications of supercritical water for energy and the environment, ChemSusChem 1 (2008) 486–503.
[16] S. Wang, D. Xu, Y. Guo, Supercritical Water Processing Technologies for Environment, Energy and Nanomaterial Applications, Springer Nature, Singapore, 2020.
[17] J.B. Gadhe, R.B. Gupta, Hydrogen production by methanol reforming in supercritical water: suppression of methane formation, Ind. Eng. Chem. Res. 44 (2005) 4577–4585.
[18] D. Castello, Supercritical Water Gasification of Biomass, Dissertation. Trento, Italy, 2013.
[19] M. Schubert, J.W. Regler, F. Vogel, Continuous salt precipitation and separation from supercritical water. Part 1: type 1 salts, J. Supercrit. Fluids 52 (2010) 99–112.
[20] F.J. Armellini, Phase Equilibria and Precipitation Phenomena of Sodium Chloride and Sodium Sulfate in Sub- and Supercritical Water, Dissertation, Cambridge, USA, 1993.
[21] N. Boukis, A. Kruse, U. Galla, V. Diem, E. Dinjus, Biomassevergasung in überkritischem wasser, Nachrichten Forschungszentrum Karlsr. 35 (2003) 99–104.
[22] C. Wang, C. Zhu, J. Huang, H. Jin, X. Lian, Gasification of biomass model compounds in supercritical water: detailed reaction pathways and mechanisms, Int. J. Hydrogen Energy 74 (2022) 31843–31851.

[23] F.L.P. Resende, P.E. Savage, Kinetic model for noncatalytic supercritical water gasification of cellulose and lignin, AIChE J. 56 (2010) 2412–2420.
[24] Q. Guan, C. Wei, P.E. Savage, Kinetic model for supercritical water gasification of algae, Phys. Chem. Chem. Phys. 14 (2012) 3140–3147.
[25] M.H. Waldner, F. Vogel, Renewable production of methane from woody biomass by catalytic hydrothermal gasification, Ind. Eng. Chem. Res. 44 (2005) 4543–4551.
[26] J. Yu, P.E. Savage, Decomposition of formic acid under hydrothermal conditions, Ind. Eng. Chem. Res. 37 (1998) 2–10.
[27] J.A. Okolie, R. Rana, S. Nanda, A.K. Dalai, J.A. Kozinski, Supercritical water gasification of biomass: a state-of- the-art review of process parameters, reaction mechanisms and catalysis, Sustain. Energy Fuels 3 (2019) 578–598.
[28] N. Boukis, I.K. Stoll, Gasification of biomass in supercritical water, challenges for the process design—lessons learned from the operation experience of the first dedicated pilot plant, Processes 9 (2021) 1–17.
[29] R.F. Susanti, B. Veriansyah, J.-D. Kim, J. Kim, Y.-W. Lee, Continuous supercritical water gasification of isooctane: a promising reactor design, Int. J. Hydrogen Energy 35 (2010) 1957–1970.
[30] D. Yu, M. Aihara, M.J. Antal Jr., Hydrogen production by steam reforming glucose in supercritical water, Energy Fuel. 7 (1993) 574–577.
[31] N. Boukis, U. Galla, H. Müller, E. Dinjus, Die VERENA-Anlage - erzeugung von Wasserstoff aus Biomasse. Gülzower Fachgespräche, Band 25, Wasserstoff aus Biomasse, Fachagentur Nachwachsende Rohstoffe e.V 115–27 (2006).
[32] M Modell, RC Reid, SI Amin. Gasifiaction Process: Patent US4113446, A, 1978.
[33] N. Boukis, V. Diem, W. Habicht, E. Dinjus, Methanol reforming in supercritical water, Ind. Eng. Chem. Res. 42 (2003) 728–735.
[34] J. Dutzi, A.A. Vadarlis, N. Boukis, J. Sauer, Comparison of experimental results with thermodynamic equilibrium simulations of supercritical water gasification of concentrated ethanol solutions with focus on water splitting, Ind. Eng. Chem. Res. 62 (32) (2023) 12501–12512.
[35] N. Boukis, U. Galla, H. Müller, E. Dinjus, Biomass Gasification in Supercritical Water. Experimental progress achieved with the VERENA pilot plant, in: Proceedings of 15th European Biomass Conference & Exhibition, 2007. Berlin, Germany, 7-11 May.
[36] P.R. Rout, D.S. Pandey, M. Haynes-Parry, C. Briggs, H.L.C. Manuel, R. Umapathi, et al., Ustainable valorisation of animal manures via thermochemical conversion technologies: an inclusive review on recent trends, Waste and Biomass Valorization 14 (2023) 553–582.
[37] W. Su, M. Zhao, Y. Xing, H. Ma, P. Liu, X. Li, et al., Supercritical water gasification of hyperaccumulators for hydrogen production and heavy metal immobilization with alkali metal catalysts, Environ. Res. 214 (2022) 1–10.
[38] O. Sawai, T. Nunoura, K. Yamamoto, Supercritical water gasification of sewage sludge using bench-scale batch reactor: advantages and drawbacks, J. Mater. Cycles Waste Manag. 16 (2014) 82–92.
[39] J. Lin, S. Sun, C. Cui, R. Ma, L. Fang, R. Zhang, et al., Hydrogen-rich bio-gas generation and optimization in relation to heavy metals immobilization during Pd-catalyzed supercritical water gasification of sludge, Energy 189 (2019).
[40] L. Li, W. Cao, G. Wang, P. Peng, S. Liu, H. Jin, et al., Experimental and kinetic study of heavy metals transformation in supercritical water gasification of oily sludge, J. Clean. Prod. (2022) 373.
[41] A. Chuntanapum, Y. Matsumura, Char Formation mechanism in supercritical water gasification process: a study of model compounds, Ind. Eng. Chem. Res. 49 (2010) 4055–4062.
[42] S.N. Reddy, S. Nanda, A.K. Dalai, J.A. Kozinski, Supercritical water gasification of biomass for hydrogen production, Int. J. Hydrogen Energy 39 (2014) 6912–6926.
[43] L.J. Guo, Y.J. Lu, X.M. Zhang, C.M. Ji, Y. Guan, A.X. Pei, Hydrogen production by biomass gasification in supercritical water: a systematic experimental and analytical study, Catal. Today 129 (2007) 275–286.
[44] R.A. Lord, Reed canarygrass (Phalaris arundinacea) outperforms Miscanthus or willow on marginal soils, brownfield and non-agricultural sites for local, sustainable energy crop production, Biomass Bioenergy 78 (2015) 110–125.
[45] A. Sinag, A. Kruse, V. Schwarzkopf, Key compounds of the hydropyrolysis of glucose in supercritical water in the presence of K2CO3, Ind. Eng. Chem. Res. 42 (2003) 3516–3521.
[46] A. Sinag, A. Kruse, J. Rathert, Influence of the heating rate and the type of catalyst on the formation of key intermediates and on the generation of gases during hydropyrolysis of glucose in supercritical water in a batch reactor, Ind. Eng. Chem. Res. 43 (2004) 502–508.
[47] Z. Zhu, S.S. Toor, L.A. Rosendahl, D. Yu, G. Chen, Influence of alkali catalyst on product yield and properties via hydrothermal liquefaction of barley straw, Energy 80 (2015) 284–292.
[48] K. Saritpongteeraka, J. Kaewsung, B. Charnnok, S. Chaiprapat, Comparing low-temperature hydrothermal pretreatments through convective heating versus microwave heating for napier grass digestion, Processes 8 (2020) 1221.
[49] T. Zheng, K. Zhang, X. Chen, Y. Ma, B. Xiao, J. Liu, Effects of low- and high-temperature thermal-alkaline pretreatments on anaerobic digestion of waste activated sludge, Bioresour. Technol. 337 (2021) 125400.
[50] B. Dokbua, N. Waramit, J. Chaugool, C. Thongjoo, Biomass productivity, developmental morphology, and nutrient removal rate of hybrid napier grass (Pennisetum purpureum x Pennisetum americanum) in response to potassium and nitrogen fertilization in a multiple-harvest system, Bioenerg. Res. 14 (2021) 1106–1117.
[51] I.Y. Mohammed, Y.A. Abakr, F.K. Kazi, S. Yusup, I. Alshareef, S.A. Chin, Comprehensive characterization of napier grass as a feedstock for thermochemical conversion, Energies 8 (2015) 3403–3417.
[52] P. D'Jesus, N. Boukis, B. Kraushaar-Czarnetski, E. Dinjus, Gasification of corn and clover grass in supercritical water, Fuel 85 (2006) 1032–1038.
[53] O. Yakaboylu, I. Albrecht, J. Harnick, K.G. Smit, G.-A. Tsalidis, M.D. Marcello, et al., Supercritical water gasification of biomass in fluidized bed: first results and experiences obtained from TU Delft/Gensos semi-pilot scale setup, Biomass Bioenergy 111 (2018) 330–342.
[54] L.J. Sealock, D.C. Elliott, E.G. Baker, R.S. Butner, Chemical processing in high-pressure aqueous environments. 1. Historical perspective and continuing developments, Ind. Eng. Chem. Res. 32 (1993) 1535–1541.
[55] N. Boukis, U. Galla, P. D'Jesús, H. Müller, E. Dinjus, Gasification of wet biomass in supercritical water. Results of pilot plant experiments, in: Proceedings of 14th European Biomass Conference for Energy, Industry and Climate Protection, Paris, France, October 2005, pp. 17–21.
[56] M. Hodes, P.A. Marrone, G.T. Hong, K.A. Smith, J.W. Tester, Salt precipitation and scale control in supercritical water oxidation—Part A. Fundamentals and research, J. Supercrit. Fluids 29 (2004) 265–288.
[57] A. Kruse, Supercritical water gasification, Biofuels, Bioprod., Bioref. 2 (2008) 415–437.
[58] P. Kritzer, N. Boukis, E. Dinjus, Factors controlling corrosion in high-temperature aqueous solutions. A contribution to the dissociation and solubility data influencing corrosion processes, J. Supercrit. Fluids 15 (1999) 205–227.
[59] N. Boukis, W. Habicht, E. Hauer, K. Weiss, E. Dinjus, Corrosion behavior of Ni-base alloys and stainless steels in supercritical water containing potassium hydrogen carbonate, in: Proceedings of the EUROCORR 2008 the European Corrosion Congress, 2008. Edinburgh, UK, 7 – 11 September.
[60] M. Schubert, Catalytic Hydrothermal Gasification of Biomass - Salt Recovery and Continous Gasifiaction of Glycerol Solutions, Dissertation. Zurich, Switzerland, 2010.
[61] V. Valyashko, Phase behaviour in binary and ternary water-salt systems at high temperatures and pressures, Pure Appl. Chem. 69 (1997) 2271–2280.
[62] U. Ekpo, A.B. Ross, M.A. Camargo-Valero, P.T. Williams, A comparison of product yields and inorganic content in process streams following thermal hydrolysis and hydrothermal processing of microalgae, manure and digestate, Bioresour. Technol. 200 (2016) 951–960.
[63] L. Zhao, J. Zhang, C.D. Sheng, K. Wang, Q.Z. Ding, Dissolution characteristics of inorganic elements existing in biomass during the supercritical water gasification process, Energy Sources, Part A Recovery, Util. Environ. Eff. 34 (2012) 1893–1900.
[64] T. Yanagida, T. Minowa, A. Nakamura, Y. Matsumura, Y. Noda, Behavior of inorganic elements in poultry manure during supercritical water gasification, J. Jpn. Inst. Energy 87 (2008) 731–736.
[65] H. Weingärtner, E.U. Franck, Überkritisches Wasser als Lösungsmittel, Angew. Chem. 117 (2005) 2730–2752.
[66] P. D'Jesus, Die Vergasung von realer Biomasse in überkritischem Wasser: Untersuchung des Einflusses von Prozessvariablen und Edukteigenschaften, Dissertation. Karlsruhe, Germany, 2007.
[67] G. Cheng, J. Andries, Z. Luo, H. Spliethoff, Biomass pyrolysis/gasification for product gas production: the overall investigation of parametric effects, Energy Convers. Manag. 44 (2003) 1875–1884.
[68] Y. Lu, L. Guo, X. Zhang, X. Hao, Q. Yan, Hydrogen production by biomass gasification in supercriticalwater: a parametric study, Int. J. Hydrogen Energy 31 (2006) 822–831.
[69] M. Tushar, A. Dutta, C. Xu, Effects of reactor wall properties, operating conditions and challenges for SCWG of real wet biomass, in: Z. Fang, C. Xu (Eds.), Near-critical and Supercritical Water and Their Applications: Biofuels and Biorefineries 2, Springer Science+Business Media Dordrecht, Dordrecht, Netherlands, 2014, pp. 207–229.
[70] S. Nanda, S.N. Reddy, H.N. Hunter, A.K. Dalai, J.A. Kozinski, Supercritical water gasification of fructose as a model compound for waste fruits and vegetables, J. Supercrit. Fluids 104 (2015) 112–121.